Development of LFT-based Models for Robust Stability Analysis of a generic Electrical Power System over all operating conditions

Sharmila Sumsurooah
The Department of Electrical and Electronic Engineering
The University of Nottingham
Nottingham NG7 2RD, UK
eexss23@nottingham.com

Milijana Odavic
The Department of Electronic and Electrical Engineering
The University of Sheffield
Sheffield S10 2TN, UK
M.Odavic@sheffield.ac.uk

Serhiy Bozhko
The Department of Electrical and Electronic Engineering
The University of Nottingham
Nottingham NG7 2RD, UK
Serhiy.Bozhko@nottingham.ac.uk

***Abstract*—This paper develops a method to analyse robust stability of a generic electrical power system for safe-critical applications over all operating conditions. Standard methods can guaranty stability under nominal conditions but do not take into account any uncertainties of the model. In this work, stability is assessed by using a Structural Singular Value concept that can provide a measure of stability robustness of a Linear Fractional Transformation (LFT)-based linear system with structured parametric uncertainties. In line with this, the first step was to develop a parameter-dependent linear time-invariant state-space model of the system that is valid for all operating conditions. The model was obtained by symbolic linearisation of the system non-linear model and was further extended to include structured parametric uncertainties of the system. The developed approach was successfully applied to determine the critical destabilising torque of a 4 kW permanent magnet motor drive over the defined range of operating conditions. Matlab robust stability toolbox was used for this analysis. The results were validated against simulation and experimental data.**

***Index Terms*—Robust stability, Linear fractional transformation, Structural singular value, Large signal stability analysis.**

I. Introduction

This paper addresses stability issues in aircraft electrical power systems (EPS). The More-Electric Aircraft will have an increased electrical distribution with a multiplicity of power electronics converters interfaced loads. It is well known that these loads, when tightly controlled, present a negative impedance to the source and thus can cause severe stability issues within the power system [1]. In order to be able to guaranty stability of the system over all operating conditions, uncertainties in the system model have to be taken into account.

Based on existing work on modelling symbolic non-linear equations of a generic electrical power system, the work develops Linear Fractional Transformation (LFT)-based uncertainty descriptions of the EPS for analysing stability robustness of the system with parametric uncertainties using the principle of structural singular value (SSV) also referred to as μ analysis.

The structural singular value is an approach that was proposed to analyse the robust stability of linear models with structured parametric uncertainties, described by Linear Fractional Transformation [2] [3].The strength of robust stability theory lies in the fact that it can determine the critical boundary stability condition of uncertain system models where one or multiple system parameters are allowed to vary within defined uncertainty sets. The uncertain system model is closer to the real system as it takes into account perturbations which are often not considered in designs which are based solely on nominal parameter values. Besides, where power systems are subject to perturbations, classical stability methods, such as Modal analysis method, cannot guarantee identification of all critical parameters.

Generally stability studies are based on small signal models whereby the analysis of the system behaviour is limited to the region close to the steady state operating point. In order to analyse small signal stability of the system for all operating points, the classical approach is to divide the operating range into N points and for each operating point to obtain numerical linearisation of the non-linear system model in order to calculate eigenvalues of the linearised system matrix. However, this approach cannot take into account dependences of the system operating points onto the system parametric uncertainties. Thus, the aim of our work was to develop a general approach to linearise a non-linear system model over all operating conditions and to represent the system by a unique time-invariant state space model in symbolic form with explicit parametric uncertainties suitable for μ analysis. This has been addressed through the symbolic linearisation of a non-linear system model. The approach will be illustrated by applying it to a 4 kW PM machine drive to predict the system stability margin over the defined range of operating conditions.

II. Theoretical Background

A. Overview of Uncertain Systems

Fig. 1a shows an original uncertain system M_Δ with the multiple sources of perturbations embedded in the system

978-1-4799-7400-9/15/$31.00 ©2015 IEEE

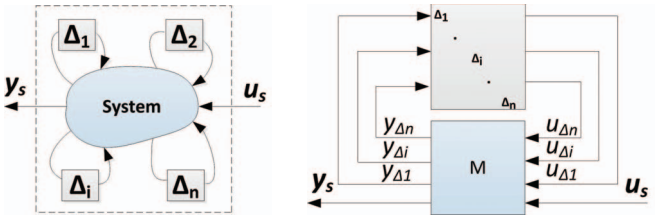

(a) Perturbations embedded in original system M_Δ

(b) Perturbations pulled out in $M\Delta$ configuration using LFT

Fig. 1: Uncertain system

[3]. It is possible to separate unknown perturbations from the known part of the system, regroup them in a diagonal matrix Δ and represent the uncertain system in an $M\Delta$ configuration as shown in Fig. 1b [3]. The $M\Delta$ model configuration enables the stability margins of uncertain systems to be assessed using SSV, as will be described later. The technique used to "pull out" the uncertainty from the system is the Linear Fractional Transformation (LFT).

This work is focused on the penetration of parameters uncertainties into the system. The state space elements $\left(\begin{smallmatrix} A & B \\ C & D \end{smallmatrix}\right)$ of an uncertain system are functions of uncertain parameters. For instance, element A_{ij} of the state matrix A can be expressed as (1) where P_1 to P_m denote uncertain parameters of the system [4]. Each uncertain parameter and consequently the whole uncertain system model can be expressed in its corresponding LFT form [5].

$$A_{ij} = f_1(P_1, P_2 ... P_m) \tag{1}$$

We will now define the structural singular value which follows the Determinant Stability Condition [6]. With the assumption that the closed loop $M\Delta$-based model in Fig.1b is initially stable, the disturbance (Δ) is gradually increased from zero. As the disturbance increases, it reaches the point where it becomes sufficiently large to cause the system to become unstable. This is the smallest structured destabilising disturbance matrix and is measured as $\overline{\sigma}(\Delta)$. The structural singular value (SSV or μ) is given by the reciprocal of the minimum value of $\overline{\sigma}(\Delta)$ at this point, which is also known as the robust stability margin when the poles are at the imaginary axis i.e. $det(I - M\Delta(jw)) = 0$, as defined in (2). The μ value also depends on the structure of Δ which explains the designation $\mu_\Delta(M(s))$. This aspect will not be pursued in this work but further information can be found in the literature [5]- [7].

$$\mu_\Delta(M(s)) = \frac{1}{min[\bar{\sigma}(\Delta) : det(I - M(s)\Delta) = 0, \Delta structured]} \tag{2}$$

The μ value is bounded by a lower and an upper limit. The upper bound gives only a sufficient condition for robustness while the lower bound gives a necessary and sufficient condition and is a measure of the critical delta matrix at the boundary of the system stability [8].

The lower bound tells us under which conditions the system becomes unstable and is given by the reciprocal of the smallest $\overline{\sigma}(\Delta)$. The lower bound of μ is equal to 1 at the robust stability margin. The smallest destabilising uncertainty $\overline{\sigma}(\Delta)$ is equal to 1 at this point. When the lower bound has a value larger than 1, the system is not robustly stable, i.e. it will not remain stable over the whole range of defined uncertainty while if its value is smaller than 1, the system is robustly stable. In this work, we will mainly work with the lower bound which will be denoted by μ in later sections.

III. Linearisation over all operating conditions

In this work, we aim to represent a non-linear system into a linear state space symbolic configuration with all elements of the system matrices expressed in an explicit parametric form valid for all operating conditions. This has been addressed through the development of the concept of symbolic linearisation. The methodology will be developed and illustrated by applying it to the PM machine drive in this section.

A. The System model

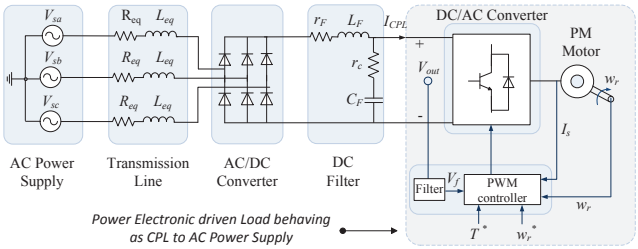

Fig. 2: The power system of the PM machine drive

We should first start with a good circuit representation of the system under study. Fig. 2 shows the main elements of one of the AC-DC distribution systems of a generic aircraft power system [9]. The engine generator with the generator control unit (GCU) assumed to have an infinitely fast controller is represented by an ideal 3-phase balanced voltage source. The transmission line from the power supply to the rectifier is modelled by an RL circuit. A six-pulse diode uncontrolled rectifier, which is an approximation of the more accepted 12-pulse rectifier in the aerospace industry, provides DC power to the electromechanical actuator (EMA) for a surface mount permanent magnet (PM) machine through a DC-link filter. The EMA of the aircraft system is a standard motor drive vector-control structure for a PM machine, depicted in Fig. 3 [9].

With the assumption that the amplitude of the AC supply and the DC load current are constant and that commutation occurs only once during a commutation period, the power stage in Fig. 2 has been modelled as the circuit in Fig. 4 by using the average-value modelling method where the six-pulse diode rectifier is represented as a DC bus voltage (V_e). The average modelling method has been developed in many publications for example in [10] and will not be derived in this work. The DC voltage V_e, the equivalent resistance R_e and

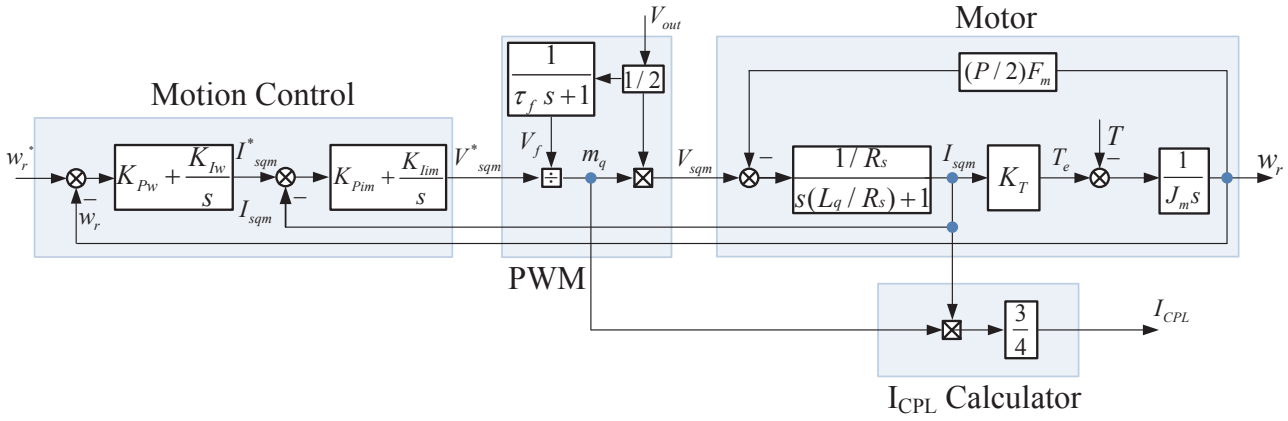

Fig. 3: Block diagram of the non-linear EMA model for PM machine

the equivalent inductance L_e are given by equations (3) to (5) where V_s is the rms value of the AC phase voltage. It is to be pointed out that the transmission line inductor L_{eq} causes an overlap angle and hence a commutation voltage drop which can be represented on the DC side by a system frequency dependent resistance r_μ as shown in equation (6).

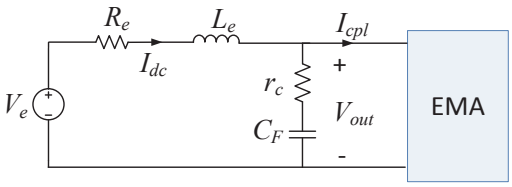

Fig. 4: Average value modelling based equivalent circuit

$$V_e = \frac{3\sqrt{3}\sqrt{2}V_s}{\pi} \quad (3)$$

$$R_e = r_\mu + r_F + 1.824R_{eq} \quad (4)$$

$$L_e = L_F + 1.824L_{eq} \quad (5)$$

$$r_\mu = \frac{3wL_{eq}}{\pi} \quad (6)$$

B. Symbolic linearisation of non-linear dynamic equations

The next step is the symbolic linearisation of the non-linear dynamic equations for the PM machine drive, given in equations (7) to (13), around its equilibrium point.

$$\dot{I}_{dc} = -\frac{(r_c+R_e)}{L_e}I_{dc} + \frac{3r_cV^*_{sqm}I_{sqm}}{2L_eV_{out}} - \frac{V_{out}}{L_e} + \frac{V_e}{L_e} \quad (7)$$

$$\dot{V}_{out} = \frac{I_{dc}}{C_F} - \frac{3V^*_{sqm}I_{sqm}}{2C_FV_{out}} \quad (8)$$

$$\dot{w}_r = \frac{K_T}{J_m}I_{sqm} - \frac{1}{J_m}T \quad (9)$$

$$\dot{I}_{sqm} = \frac{-PF_m}{2L_q}w_r - \frac{R_s}{L_q}I_{sqm} + \frac{V_{sqm}}{L_q} \quad (10)$$

$$\dot{V}_f = -\frac{1}{\tau_f}V_f + \frac{1}{2\tau_f}V_{out} \quad (11)$$

$$\dot{V}^*_{sqm} = -K_{Iim}I_{sqm} + K_{Iim}I^*_{sqm} - K_{Pim}\dot{I}_{sqm} + K_{Pim}\dot{I}^*_{sqm} \quad (12)$$

$$\dot{I}^*_{sqm} = -K_{Iw}w_r + K_{Iw}w^*_r - K_{Pw}\dot{w}_r + K_{Pw}\dot{w}^*_r \quad (13)$$

The linearised equations are then converted into the state space configuration where x, u, y are the states, input and output. The steady state variables and steady state inputs at the nominal operating point are denoted as X_o and U_o respectively. The variables of x, u, y, X_o and U_o are listed below. The symbolic parametric expressions of X_o can be obtained by equating the non-linear equations (7) to (13) to zero. The input V_e and w^*_r have constant values over all operating points while input torque varies and is denoted as T_o at steady state. It is to be noted that the voltage across the DC-Link capacitor was assumed to be equal to V_{out} given that the voltage drop across the ESR of the capacitor is very small.

- x : I_{dc}, V_{out}, w_r, I_{sqm}, V_f, V^*_{sqm}, I^*_{sqm}
- u :V_e, w^*_r, T
- y :V_{out}
- X_o: I_{dco}, V_{outo}, w_{ro}, I_{sqmo}, V_{fo}, V^*_{sqmo}, I^*_{sqmo}
- U_o :V_e, w^*_r, T_o

C. Express the state space matrix elements explicitly in terms of system inputs and other system parameters

After obtaining the linearised model, all the elements in its state space matrix have to be expressed explicitly in terms of system inputs and other system parameters. For instance, for our example circuit of the PM machine drive, the steady state variables I_{dco}, V_{outo}, w_{ro}, I_{sqmo}, V_{fo}, V^*_{sqmo}, I^*_{sqmo} were expressed in terms of T_o, w^*_r, V_e and K_T, P, F_m, R_s, R_e, η as shown in (14) to (19). Using the energy conservation conditions, $P_{dc} = 3P_{dq}/2$ where P_{dq} is the power in the *dq* frame, I_{dco} which is equal to I_{CPLo} has been derived as (14). The expression of V_{outo} in (18) is based on the constant power

load equation $I_{cplo} = P_o/V_{outo}$ where $P_o = T_o w_{ro}/\eta$ and the efficiency of the PM machine $\eta = 0.89$.

$$I_{dco} = \frac{(3T_o/2K_T)(R_s T_o/K_T + PF_m w_{ro}/2)}{V_{outo}} \quad (14)$$

$$I_{sqmo} = I^*_{sqmo} = T_o/K_T \quad (15)$$

$$V_{fo} = V_{outo}/2 \quad (16)$$

$$V^*_{sqmo} = V_{sqmo} = R_s T_o/K_T + PF_m w_{ro}/2 \quad (17)$$

$$\textit{where} \quad V_{outo} = \frac{V_e}{2}[1 + \sqrt{1 - \frac{4R_e T_o w_{ro}}{\eta V_e^2}}] \quad (18)$$

$$w_{ro} = w^*_r \quad (19)$$

D. Approximate irrational terms using polynomial expansion

All the elements in the linearised system matrix have to be in their rational form so that their parameters can be expressed in their LFT configuration. Hence, all irrational terms have to be estimated to satisfactory accuracy as a sum of rational terms by using polynomial expansion such as Taylor series expansion. In our case, the non-rational expression of V_{outo} in (18) has been estimated in its rational form in (20) by using the first two terms of the binomial expansion of the square root term in (18). (20) is a good approximation of V_{outo} with respect to variations in torque as shown in Fig. 5. Taylor's series approximation with high orders may have to be used for more complex cases. However this tends to increase the complexity of the final state space matrix and the order of the delta matrix, resulting in additional computational burden and higher simulation time.

$$V_{outo-est} = V_e - \frac{R_e T_o w_{ro}}{\eta V_e} \quad (20)$$

E. Replace the linearised state space matrix elements by their explicit rational expressions

The final step is to replace the elements in the state space matrix by their equivalent explicit rational expressions. In our case, V_{outo} is to be replaced by (20) and the other steady state variables by (14) to (17) and (19). We have thus obtained a linear time-invariant state space symbolic model with explicit rational parameters representing with good accuracy all linearisations of the non-linear model over all operating conditions. The matrix A of the developed model is shown below. The expressions for the symbols A_{subs1} and A_{subs2} which are used in matrix A are given in equations (21) and (22) respectively. It is to be pointed out that all four state space matrices A,B,C and D are required for μ analysis. The developed model can now be used for robust stability analysis of the PM machine drive over all operating conditions.

$$A_{susb1} = \frac{R_s T_o}{K_T} + \frac{PF_m w_{ro}}{2} \quad (21)$$

$$A_{subs2} = -K_{Iim} - \frac{K_{Pim} K_{Pw} K_T}{J_m} + \frac{K_{Pim} R_s}{L_q} \quad (22)$$

TABLE I: Nominal values for System parameters

Parameters	Units	Nominal Values	Description
V_s	V_{rms-ph}	223	phase source voltage
w	rad/s	2π50	source frequency
R_{eq}	Ω	0.045	line resistance
L_{eq}	μH	60	line inductance
r_F	Ω	0.2	DC-link inductor resistance
L_F	mH	24.15	DC-link inductor
r_c	Ω	0.4	ESR of DC-link capacitor
C_F	μF	320	DC-link capacitor
w_{rated}	rpm	1140	rated speed
w^*_r	rpm	800	speed reference
T_{rated}	Nm	40	rated load torque
R_s	Ω	0.5	stator resistance
L_q	mH	2.3	stator leakage inductance
P	poles	20	number of poles
J_m	kgm^2	0.004	moment of inertia
F_m	Wb	0.123	constant flux of PM machine
K_{Pim}	-	4.124	current loop PI constant
K_{Iim}	-	3632	current loop PI constant
K_{Pw}	-	0.02	speed loop PI constant
K_{Iw}	-	0.863	speed loop PI constant

TABLE II: Uncertain parameter value

Parameter	Unit	Nominal Value (T_o)	Range of variation wrt nominal value (T_{var})
T_o (torque)	Nm	20	± 90 %

IV. Robust Stability Analysis

In this section, robust stability analysis will be applied to determine the critical destabilising load torque for the system shown in Fig.2. In this analysis, all the system parameters are assumed to be constant and equal to their nominal values as defined in Table I. The only varying variable is the load torque and it can vary up to $T_{var} = \pm 90\%$ around its nominal value of T_o = 20 Nm, as defined in Table II.

A. Modelling of uncertainties

Prior to applying μ analysis, the developed linearised system model has to be converted in the equivalent $M\Delta$ form. The first step is to express all the uncertain parameters of the system matrix in their LFT form. In our case the uncertain element T_o has been expressed in its LFT form in (23) where T_{oo} is the nominal value, T_{var} is the range of variation of T_o expressed as a percentage of T_{oo} and δ_T is the unknown normalized perturbation in torque which lies between -1 and 1 [2]. T_{oo} and T_{var} are derived from the minimum torque (T_{min}) and the maximum torque(T_{max}) as shown in (25) and (26).

$$T_o = T_{oo} + T_o T_{var} \delta_T \quad (23)$$

$$-1 \leq \delta_T \leq 1 \quad (24)$$

$$T_{oo} = (T_{max} + T_{min})/2 \quad (25)$$

$$T_{var} = (T_{max} - T_{min})/(T_{max} + T_{min}) \quad (26)$$

From Fig.6, which is an illustration of equation (23), we can see that when the 'perturbation' in torque is absent, $\delta_T = 0$,

$$A = \begin{bmatrix} -\frac{r_c + R_e}{L_e} & -\frac{1}{L_e} & 0 & \frac{3r_cA_{susb1}}{2L_e\mathbf{V_{outo-est}}} & -\frac{3r_cA_{susb1}(T_o/K_T)}{L_e\mathbf{V^2_{outo-est}}} & \frac{3r_c(T_o/K_T)}{2L_e\mathbf{V_{outo-est}}} & 0 \\ \frac{1}{C_F} & 0 & 0 & \frac{-3A_{susb1}}{2C_F\mathbf{V_{outo-est}}} & \frac{3A_{susb1}(T_o/K_T)}{C_F\mathbf{V^2_{outo-est}}} & \frac{-3(T_o/K_T)}{2C_F\mathbf{V_{outo-est}}} & 0 \\ 0 & 0 & 0 & \frac{K_T}{J_m} & 0 & 0 & 0 \\ 0 & \frac{A_{susb1}}{L_q\mathbf{V_{outo-est}}} & \frac{-PF_m}{2L_q} & \frac{-R_s}{L_q} & \frac{-2A_{susb1}}{L_q\mathbf{V_{outo-est}}} & \frac{1}{L_q} & 0 \\ 0 & \frac{1}{2\tau_f} & 0 & 0 & -\frac{1}{T_f} & 0 & 0 \\ 0 & \frac{-K_{Pim}A_{susb1}}{L_q\mathbf{V_{outo-est}}} & (-K_{Pim}K_{Iw} + \frac{K_{Pim}PF_m}{2L_q}) & A_{subs2} & \frac{2K_{Pim}A_{susb1}}{L_q\mathbf{V_{outo-est}}} & \frac{-K_{Pim}}{L_q} & K_{Iim} \\ 0 & 0 & -K_{Iw} & \frac{-K_{Pw}K_T}{J_m} & 0 & 0 & 0 \end{bmatrix}$$

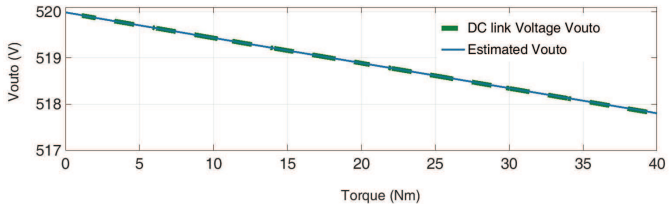

Fig. 5: Polynomial estimation of the steady state variable V_{outo}

torque equals to its nominal value of $T_o = T_{oo} = 20$Nm. When the 'perturbation' is at its maximum, either $\delta_T = -1$ at the low end of the uncertainty range where $T_o = T_{min} = 2$ Nm or $\delta_T = 1$ at the high end of the uncertainty range where $T_o = T_{max} = 38$ Nm.

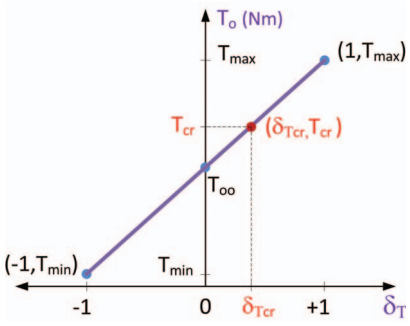

Fig. 6: Relationship between torque and the normalised disturbance in torque

After the uncertain parameters have been expressed in their LFT form, the software MATLAB Robust stability toolbox, can then be used for the automatic conversion of the uncertain system model into the normalised $M\Delta$ structure and for the computation of the lower and upper bounds of the SSV [11].

B. Application of SSV

The uncertainty matrix Δ in the $M\Delta$ configuration of the PM machine is a (24 $\times$ 24) diagonal matrix with all the diagonal elements being equal to δ_T; "24" corresponds to the number of times the uncertain element T_o appears in the system matrix and δ_T is the unknown disturbance in T_o. In order to determine the critical torque using structural singular value theory, Δ is increased gradually from zero until it reaches the point at which the system becomes unstable. This is the minimum destabilising disturbance matrix denoted as Δ_{Tcr}. In our case, the smallest $\overline{\sigma}(\Delta_{Tcr})$ is equal to δ_{Tcr} which is shown in Fig. 6. Hence, the lower bound (μ) is equal to the reciprocal of δ_{Tcr} as given in (27) [11] [12]. From the μ or δ_{Tcr} value, the critical destabilising torque T_{cr} can then be derived from (28).

$$\delta_{Tcr} = 1/\mu \quad (27)$$

$$T_{cr} = T_{oo} + T_{oo}T_{var}\delta_{Tcr} \quad (28)$$

The μ analysis of our uncertain model produced the μ chart in Fig. 7 which shows μ to be equal to 2.38 at a frequency of 57 Hz. The critical frequency of 57 Hz corresponds to the resonant frequency of the DC-link LC filter which can be determined from $1/2\pi\sqrt{L_FC_F}$. The critical uncertainty matrix Δ_{Tcr}, which was also extracted from the μ analysis, is a (24 $\times$ 24) diagonal matrix with each of the diagonal elements being equal to $\delta_{Tcr} = +0.42$. Based on the critical value δ_{Tcr} and the known values of T_{oo} and T_{var} from Table II, the critical destabilising torque T_{cr} can be determined 27.6 Nm from equation (28).

$\mu > 1$ indicates that the system is not robustly stable. The system will not remain stable over the whole defined uncertainty set which is 20$\pm$ 18 Nm but only from $T_{min} = 2$ Nm up to $T_{cr} = 27.6$ Nm. In this way, μ operates as a measure of the robustness of the system stability .

In order to ensure that our system remains stable for the whole uncertainty range, μ or the minimum value of δ_{Tcr} should be equal to 1. The first way to do this is to limit the operating range of the system to $\pm$ 7.6 Nm i.e. $T_o = 20 \pm 38\%$. If we want to maintain the operation range to $20Nm \pm 90\%$, then uncertainties in the L_F, C_F filter can be modelled in order to find their optimal values that will guaranty stability of the system in the whole operating range.

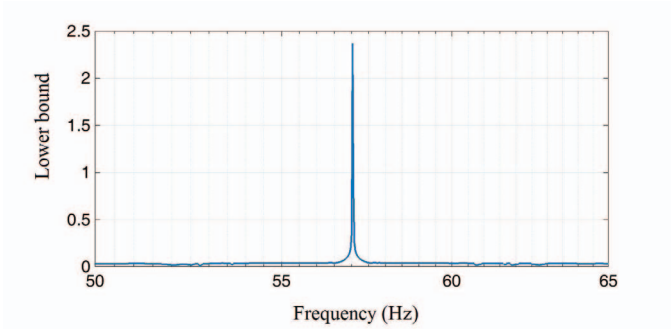

Fig. 7: μ chart for the determination of critical torque

V. Simulation Results

The PM machine drive was also modelled in the Simulink environment to enable time-domain verification of the result from μ analysis. With the speed kept constant at 800 rpm, three values of torque were applied in steps to the model. At time $t = 4$ s, 95 % of the critical torque (26.22 Nm) was applied to the system and the DC link voltage V_{out} stabilised with time as can be seen in Fig. 8. At time $t = 8$ s, application of the critical torque $T_{cr} = 27.6$ Nm caused the system to reach boundary stability with sustained DC-Link voltage oscillation. This confirms the results from μ analysis which predicted the critical torque of 27.6 Nm. Applying 5% additional torque over the critical value at $t = 12$s caused the system to become unstable as shown in Fig. 8.

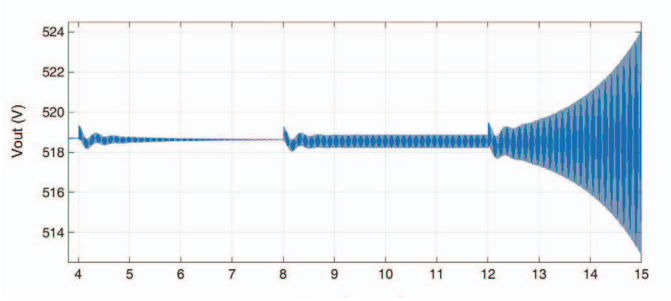

Fig. 8: Simulation DC-Link voltage V_{out} at (i) t=4s, $T = 0.95T_{cr}$ (ii) t=8s, $T = T_{cr}$(iii) t=12s, $T = 1.05T_{cr}$

VI. Experimental Results

In [9], a number of experiments were undertaken on the rig of the PM machine drive which was described in this work. It was found in the experiment that when the torque was increased to 26.72 Nm at a speed of 800 rpm, the DC-Li nk voltage waveforms showed sustained oscillation with peak-to-peak value of 80V [9] [13]. This is in very close agreement with the critical torque of 27.6 Nm determined from μ analysis. The approach developed in this work to determine the stability margin of the system over all defined operating conditions using the principle of SSV has thus been verified and validated against simulation results and experimental data of the PM machine drive.

VII. Conclusion

The aim of this work was to apply robust stability analysis to determine the robust stability margins of a non-linear model of an electrical power system over all operating conditions. The objective was met through the development of the modelling approach which involved the representation of the non linear model into a linear state space explicit parametric form that is valid for the whole operating range and can account for uncertainties in system parameters. The approach was successfully applied to determine the critical destabilising torque of a 4 kW permanent magnet motor drive over its defined range of operation. The results from robust stability analysis were validated against results from time domain simulations and experimental data.

Acknowledgment

The authors gratefully acknowledge the support for the work from the EU as part of the Clean Sky project, part of EU FP7 program.

References

[1] A. B. Jusoh, "The instability effect of constant power loads," in *Power and Energy Conference, 2004. PECon 2004. Proceedings. National*, pp. 175–179, IEEE, 2004.

[2] S. Sumsurooah, M. Odavic, and D. Boroyevich, "Modelling and robust stability analysis of uncertain systems," in *Proceedings of the 2013 Grand Challenges on Modeling and Simulation Conference*, p. 13, Society for Modeling & Simulation International, 2013.

[3] S. Skogestad and I. Postlethwaite, *Multivariable Feedback Control: Analysis and Design*. Multivariable Feedback Control: Analysis and Design, Wiley, 2005.

[4] R. Castellanos, A. Messina, and H. Sarmiento, "Robust stability analysis of large power systems using the structured singular value theory," *International Journal of Electrical Power & Energy Systems*, vol. 27, no. 5, pp. 389–397, 2005.

[5] K. Zhou, J. Doyle, and K. Glover, *Robust and Optimal Control*. Feher/Prentice Hall Digital and, Prentice Hall, 1996.

[6] J. Doyle, "Analysis of feedback systems with structured uncertainties," in *IEE Proceedings D (Control Theory and Applications)*, vol. 129, pp. 242–250, IET, 1982.

[7] M. Green and D. J. Limebeer, *Linear robust control*. Courier Dover Publications, 2012.

[8] A. Packard and J. Doyle, "The complex structured singular value," *Automatica*, vol. 29, no. 1, pp. 71–109, 1993.

[9] K. Areerak, S. Bozhko, G. Asher, L. De Lillo, and D. Thomas, "Stability study for a hybrid ac-dc more-electric aircraft power system," *Aerospace and Electronic Systems, IEEE Transactions on*, vol. 48, no. 1, pp. 329–347, 2012.

[10] S. Sudhoff and O. Wasynczuk, "Analysis and average-value modeling of line-commutated converter-synchronous machine systems," *Energy Conversion, IEEE Transactions on*, vol. 8, no. 1, pp. 92–99, 1993.

[11] G. J. Balas, J. C. Doyle, K. Glover, A. Packard, and R. Smith, "$\{/mu\}$-analysis and synthesis toolbox: For use with {MATLAB}," 2001.

[12] D.-W. Gu, *Robust Control Design with MATLAB*, vol. 1. Springer, 2005.

[13] K. Areerak, *Modelling and stability analysis of aircraft power systems*. PhD thesis, University of Nottingham, 2009.